

2HDM at the LHC - the story so far

A. Barroso

*Centro de Física Teórica e Computacional, Faculdade de Ciências,
Universidade de Lisboa, Av. Prof. Gama Pinto 2, 1649-003 Lisboa, Portugal*

P.M. Ferreira* and Rui Santos†

*Instituto Superior de Engenharia de Lisboa - ISEL, 1959-007 Lisboa, Portugal and
Centro de Física Teórica e Computacional, Faculdade de Ciências,
Universidade de Lisboa, Av. Prof. Gama Pinto 2, 1649-003 Lisboa, Portugal*

Marc Sher

High Energy Theory Group, College of William and Mary, Williamsburg, Virginia 23187, U.S.A.

João P. Silva‡

*Instituto Superior de Engenharia de Lisboa, 1959-007 Lisboa, Portugal and
Centro de Física Teórica de Partículas (CFTP), Instituto Superior Técnico,
Universidade Técnica de Lisboa, 1049-001 Lisboa, Portugal*

We confront the most common version of the CP-conserving 2HDM with LHC data, taking into account all previously available experimental data. We also discuss the scenario where the 125 GeV Higgs discovered at the LHC is the lightest neutral scalar of a particular CP-violating 2HDM. In this scenario we focus on what data can already tell us about the amount of mixing between CP-even and CP-odd states.

I. INTRODUCTION

After the discovery [1, 2] of a Higgs boson at CERN’s Large Hadron Collider (LHC), it is now time to confront possible extensions of the Standard Model (SM) with LHC data. One of the simplest ways to extend the scalar sector of the SM is to add one more complex doublet to the model. The resulting two Higgs doublet models (2HDMs) can provide additional CP-violation coming from the scalar sector and can easily originate dark matter candidates. More evolved models with additional field content have a 2HDM like scalar sector - as in the case, for instance, of the Minimal Supersymmetric Standard Model. 2HDMs have a richer particle spectrum with one charged and three neutral scalars. All neutral scalars could in principle be the scalar discovered at the LHC [3–5]. However, data gathered so far allow us to rule out the 125 GeV particle as being a pure pseudoscalar state. Hence, we are left with either one of the CP-even states of a CP-conserving model or a neutral state from a CP-violating model [6]. In the next section we will present the 2HDM models and in the following sections we discuss in turn how well 2HDMs can accommodate LHC data for the CP-conserving and for the CP-violating case.

II. THE MODELS

In this section we present the two versions of the 2HDM to be discussed, one CP-conserving and the other explicitly CP-violating. The most general 2HDMs’ Yukawa Lagrangian gives rise to scalar exchange flavour changing neutral currents (FCNCs) which are strongly constrained by experiment. A simple and natural way to avoid those dangerous FCNCs is to impose a Z_2 symmetry on the scalar doublets, $\Phi_1 \rightarrow \Phi_1$, $\Phi_2 \rightarrow -\Phi_2$, and a corresponding symmetry to the quark fields. This leads to the well known four Yukawa model types I, II, Y (III, Flipped) and X (IV, Lepton Specific) [7, 8]. The different Yukawa types are built such that only ϕ_2 couples to all fermions (type I), or ϕ_2 couples to up-type quarks and ϕ_1 couples to down-type quarks and leptons (type

*E-mail: ferreira@cii.fc.ul.pt

†E-mail: rsantos@cii.fc.ul.pt

‡E-mail: jpsilva@cftp.ist.utl.pt

II), or ϕ_2 couples to up-type quarks and to leptons and ϕ_1 couples to down-type quarks (type Y) or finally ϕ_2 couples to all quarks and ϕ_1 couples to leptons (type X).

The scalar potential in a softly broken Z_2 symmetric 2HDM can be written as

$$V(\Phi_1, \Phi_2) = m_1^2 \Phi_1^\dagger \Phi_1 + m_2^2 \Phi_2^\dagger \Phi_2 + (m_{12}^2 \Phi_1^\dagger \Phi_2 + \text{h.c.}) + \frac{1}{2} \lambda_1 (\Phi_1^\dagger \Phi_1)^2 + \frac{1}{2} \lambda_2 (\Phi_2^\dagger \Phi_2)^2 \\ + \lambda_3 (\Phi_1^\dagger \Phi_1) (\Phi_2^\dagger \Phi_2) + \lambda_4 (\Phi_1^\dagger \Phi_2) (\Phi_2^\dagger \Phi_1) + \frac{1}{2} \lambda_5 [(\Phi_1^\dagger \Phi_2)^2 + \text{h.c.}] ,$$

where Φ_i , $i = 1, 2$ are complex SU(2) doublets. All parameters except for m_{12}^2 and λ_5 are real as a consequence of the hermiticity of the potential. The phases of m_{12}^2 and λ_5 together with the ones in the vacuum expectation values (VEVs) will determine the CP nature of the model (see [9] for a review). A CP-violating model has three spin 0 neutral states usually denoted by h_1 , h_2 and h_3 while in the CP-conserving case the three CP-eigenstates are usually denoted by h and H (CP-even) and A (CP-odd). As shown in [10, 11], once either a CP-conserving or a CP-violating vacuum configuration is chosen, all charge breaking stationary points are saddle points with higher energy. Hence, the 2HDM is stable at tree-level against charge breaking and once a non-charge breaking vacuum is chosen both models have two charged Higgs bosons that complete the 2HDM particle spectrum.

We will focus on two specific realisations of 2HDMs. One is the usual 7-parameter CP-conserving potential where m_{12}^2 , λ_5 and the VEVs are all real. In this model we choose as free parameters, the four masses, the rotation angle in the CP-even sector, α , the ratio of the vacuum expectation values, $\tan \beta = v_2/v_1$, and the soft breaking parameter redefined as $M^2 = m_{12}^2/(\sin \beta \cos \beta)$. The other is an explicit CP-violating model [12–14]. In the CP-violating version m_{12}^2 and λ_5 are complex and the fields' VEVs are real. Existence of a stationary point requires $Im(m_{12}^2) = v_1 v_2 Im(\lambda_5)$. Because the VEVs are real in both models, a common definition for the rotation angle in the charged sector $\tan \beta = v_2/v_1$ can be used. In this model, besides m_{H^\pm} and $\tan \beta$, we take as free parameters the masses of the lightest scalars m_{h_1} and m_{h_2} the three rotation angles in the neutral sector α_1 , α_2 and α_3 and $Re(m_{12}^2)$. Details of the model can be found in [12–14].

A. Constraints on the models

We have imposed the following theoretical bounds on both models: we require that the potential is bounded from below [15] and we impose unitarity limits on the quartic Higgs couplings [16]. We have also taken into account the precision electroweak constraints [17, 18]. Furthermore, we discuss the scenarios in which two normal minima coexist in the CP-conserving potential. In those scenarios it could happen that we are living in a local minimum and tunnelling to a global deeper minimum could occur. This deeper minimum would have a different v^2 and therefore different masses for the elementary particles. We call this a panic vacuum [11, 19, 20]. The experimental bounds pertaining to the charged sector apply to both models since the charged Higgs Yukawa couplings have exactly the same form. Except for the LEP bounds they all constrain regions of the $(\tan \beta, m_{H^\pm})$ plane. The LEP experiments have set a lower limit on the mass of the charged Higgs boson of 80 GeV at 95% C.L., assuming $BR(H^+ \rightarrow \tau^+ \nu) + BR(H^+ \rightarrow c\bar{s}) + BR(H^+ \rightarrow A W^+) = 1$ [21] with the process $e^+ e^- \rightarrow H^+ H^-$. The bound on the mass is 94 GeV if $BR(H^+ \rightarrow \tau^+ \nu) = 1$ [21]. These are model independent bounds as long as the above mentioned sum of BRs is one. Values of $\tan \beta$ smaller than $O(1)$ together with a charged Higgs with a mass below $O(100 \text{ GeV})$ are both disallowed by the constraints [22] coming from R_b , from $B_q \bar{B}_q$ mixing and from $B \rightarrow X_s \gamma$ [23] for all models. Furthermore, data from $B \rightarrow X_s \gamma$ [23] imposes a lower limit of $m_{H^\pm} \gtrsim 360 \text{ GeV}$, but only for models type II and type Y. We have also considered the most recent bounds from the ATLAS [24] and CMS [25] collaborations on the $(\tan \beta, m_{H^\pm})$ plane coming from $pp \rightarrow t\bar{t} \rightarrow b\bar{b} W^\mp H^\pm (\rightarrow \tau \nu)$. Finally, we have considered the LEP bounds on the neutral Higgs [26].

Combining it all, our scans will be performed taking $m_{H^\pm} \geq 90 \text{ GeV}$ and $\tan \beta \geq 1$ for type I while $m_{H^\pm} > 360 \text{ GeV}$ for type II. For the CP-conserving case we also take $m_A \geq 90 \text{ GeV}$, $m_h = 125 \text{ GeV}$ and $m_H > m_h$ while α is free to vary in its allowed range although subject to the above constraints. For the CP-violating model we take $m_{h_1} = 125 \text{ GeV}$ and $m_{h_2} > m_{h_1}$ while α_i ($i = 1, 2, 3$) are again free to vary in their allowed ranges, subject to the above constraints. Finally, we note that we do not include the constraint that would result from the anomaly observed by the BaBar collaboration in the rates $R(D)$ and $R(D^*)$, with $R(D) = (\overline{B} \rightarrow D \tau^- \bar{\nu}_\tau) / (\overline{B} \rightarrow D l^- \bar{\nu}_l)$, which deviates by 3.4σ (when D and D^* final states are combined) from the SM prediction [27]. It is clear that the deviation cannot be explained by a charged Higgs boson from either of the four FCNC conserving Yukawa types. Therefore, if this observation is independently confirmed by the BELLE collaboration not only the SM will be excluded at 3.4σ but all 2HDMs Yukawa types will also be excluded with a very similar significance.

We should point out that there will never be an exclusion of the 2HDM in favor of the SM. Indeed, the models discussed here include the SM as a specific (decoupling) region of parameter space. As a result, experiments

may exclude the SM in favor of the 2HDM; they may exclude both; or they may be compatible with SM, thus restricting the 2HDM extension into a particular (eventually, small) region of the parameter space.

III. CP-CONSERVING MODEL

We start with the CP-conserving model and randomly generate points in the parameter space such that $m_h = 125$ GeV, 90 GeV $\leq m_A \leq 900$ GeV, $m_h < m_H \leq 900$ GeV, $1 \leq \tan \beta \leq 40$, $-(900)^2$ GeV² $\leq m_{12}^2 \leq 900^2$ GeV² and $-\pi/2 \leq \alpha \leq \pi/2$. Further, for type I we take 90 GeV $\leq m_{H^\pm} \leq 900$ GeV while for type II the allowed range is 360 GeV $\leq m_{H^\pm} \leq 900$ GeV. In order to use the LHC data we define the quantities R_f as the ratio of the number of events predicted in the 2HDM to that obtained in the SM for a given final state f .

$$R_f = \frac{\sigma(pp \rightarrow h)_{2\text{HDM}} \text{BR}(h \rightarrow f)_{2\text{HDM}}}{\sigma(pp \rightarrow h_{\text{SM}}) \text{BR}(h_{\text{SM}} \rightarrow f)}, \quad (1)$$

where h is the lightest CP-even Higgs (125 GeV), σ is the Higgs production cross section, BR the branching ratio, and h_{SM} is the SM Higgs boson. In our analysis, we include all Higgs production mechanisms, namely, gluon-gluon fusion using HIGLU at NLO [28], vector boson fusion (VBF) [29], Higgs production in association with either W , Z or $t\bar{t}$ [29], and $b\bar{b}$ fusion [30]. A different approach was recently followed in [31] where they have looked for the best fit point in parameter space for the four Yukawa types of the same CP-conserving 2HDM.

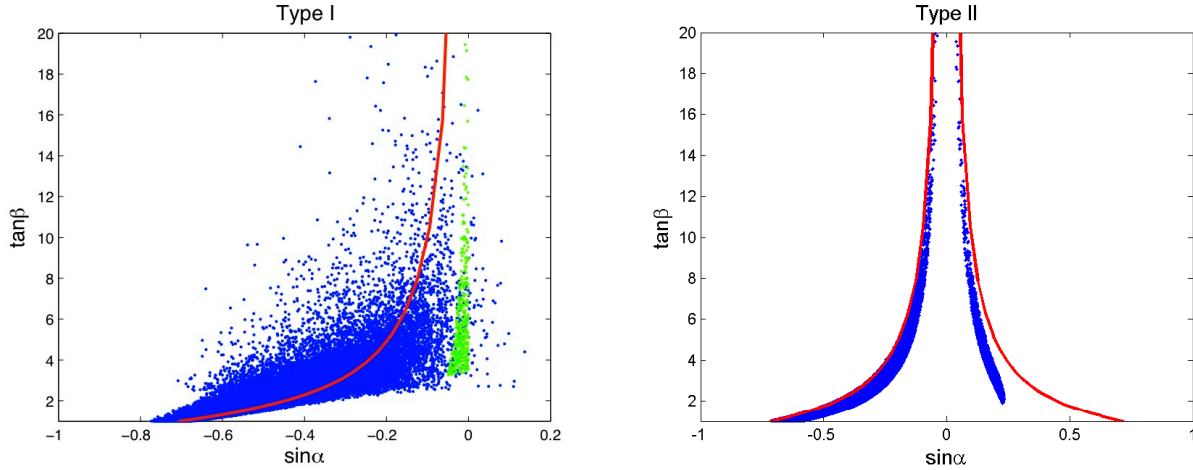


FIG. 1: Points in the $(\sin \alpha, \tan \beta)$ plane that passed all the constraints in type I (left) and in type II (right) at 1σ in green (light grey) and 2σ in blue (dark grey). Also shown are the lines for the SM-like limit, that is $\sin(\beta - \alpha) = 1$ (negative $\sin \alpha$) and for the limit $\sin(\beta + \alpha) = 1$ (positive $\sin \alpha$).

The points generated have then to pass all the constraints previously described plus the combined [32] ATLAS and CMS strengths $R_{\gamma\gamma} = 1.66 \pm 0.33$, $R_{ZZ} = 0.93 \pm 0.28$ and $R_{\tau\tau} = 0.71 \pm 0.42$. It is important to point out that this talk was given in February, 2013, prior to the updates from Moriond. We have added a subsection regarding the Moriond updates below. In figure 1 we present the points in the $(\sin \alpha, \tan \beta)$ plane that pass all the constraints in type I (left) and in type II (right) at 1σ in green and at 2σ in blue. Also shown are the lines for the SM-like limit, that is $\sin(\beta - \alpha) = 1$ (negative $\sin \alpha$) and for the limit $\sin(\beta + \alpha) = 1$ (positive $\sin \alpha$).

To better understand these results we approximate R_{ZZ} in the case where Higgs production is due exclusively to gluon-gluon fusion via the top quark loop, and the total Higgs width is well approximated by $\Gamma(h \rightarrow b\bar{b})$. This is a very good approximation for most of the parameter space and it yields

$$R_{ZZ}^{I,approx} = \frac{\cos^2 \alpha}{\sin^2 \beta} \sin^2(\alpha - \beta) \frac{\sin^2 \beta}{\cos^2 \alpha} = \sin^2(\alpha - \beta). \quad (2)$$

By setting $R_{ZZ}^{I,approx} = 1$ one obtains the SM-like limit line shown in the picture for negative α . Applying the same simplified scenario we obtain for type II

$$R_{ZZ}^{II,approx} = \sin^2(\alpha - \beta) \frac{1}{\tan^2 \alpha \tan^2 \beta}. \quad (3)$$

Now, when $R_{ZZ}^{II,approx} = 1$ we obtain not one but two lines, the red lines shown in figure 1. The approximate scenarios lead us to the following conclusions. First, it is very hard in type I to have R_{ZZ} above 1. Further, the function $\sin^2(\alpha - \beta)$ is very sensitive to deviations from 1. This leads to a larger dispersion of points around the SM-like limit line. Regarding type II, not only do we get two lines instead of one but the function $R_{ZZ}^{II,approx}$ is now very insensitive to deviations from 1 and that is why the points are all in a narrow band close to each line. It is interesting to note that while the tension between R_{ZZ} and $R_{\gamma\gamma}$ excludes all points at 1σ in type II, there is still a band in type I close to $\sin\alpha = 0$ where R_{ZZ} is below 1 while $R_{\gamma\gamma}$ can be large. The 1σ points in type I all have a charged Higgs mass below 130 GeV.

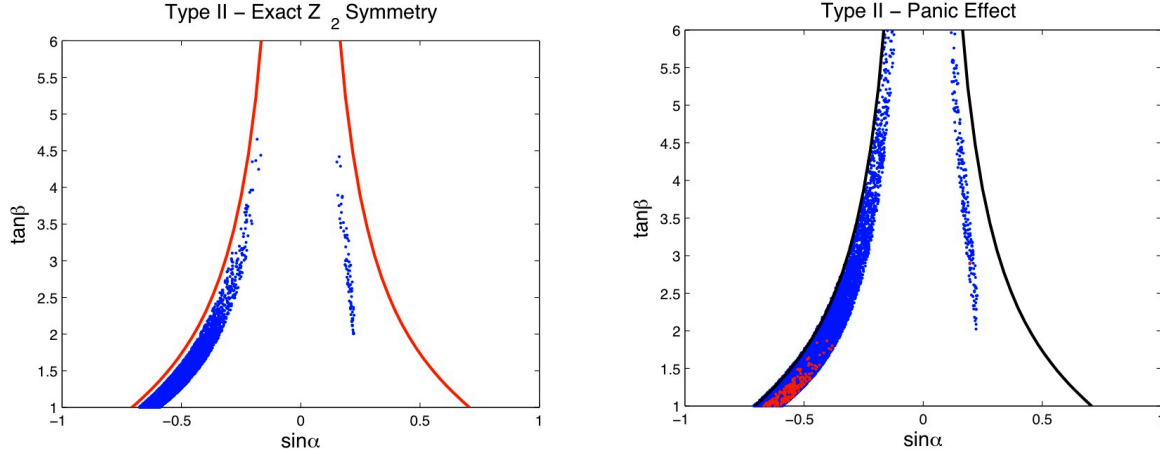


FIG. 2: In the left panel we show the points in the $(\sin\alpha, \tan\beta)$ plane that have passed all the constraints in type II with an exact Z_2 symmetry. In the right panel we show type II with the broken Z_2 symmetry where we have plotted the panic points in red. No points survive at 1σ and the 2σ points are shown in blue.

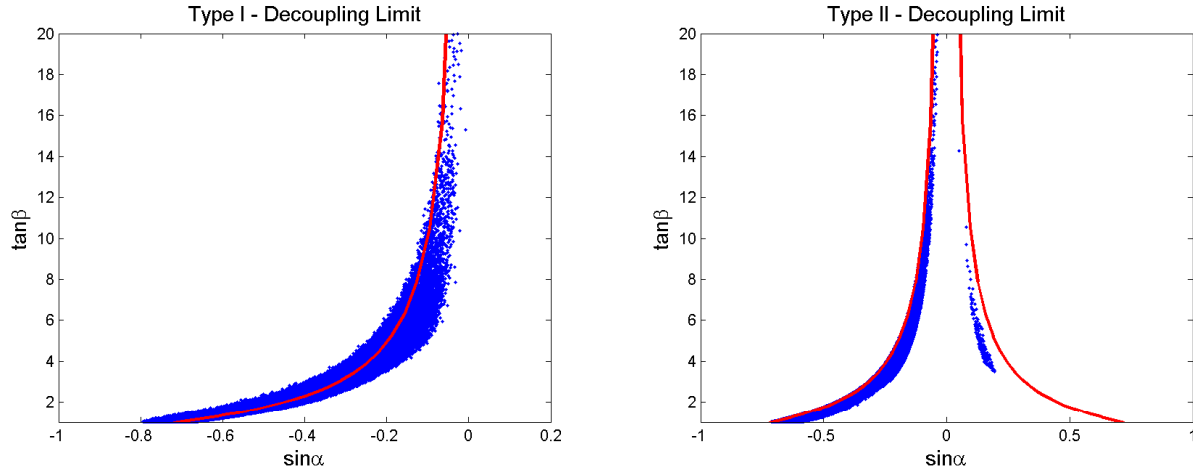


FIG. 3: Points in the $(\sin\alpha, \tan\beta)$ plane that passed all the constraints in type I (left) and in type II (right) at 2σ in blue. We have taken all masses except $m_h = 125$ GeV to be above 600 GeV.

In the left panel of figure 2 we present the points that have passed all the constraints in type II with an exact Z_2 symmetry ($m_{12}^2 = 0$). It was recently shown [33] that if $m_h = 125$ GeV, then $\tan\beta$ has to be below approximately 6. This is confirmed in the plot. Apart from the limit on $\tan\beta$, the plot does not differ much from the softly broken Z_2 case except that there are fewer points and that they move slightly away from the red lines when compared with the soft breaking scenario. We note that in type I no points survive at 1σ in the exact Z_2 symmetric case. In the right panel of figure 2 we show the panic points (in red) for the soft breaking type II model. Panic points are easily found by using the following discriminant [20]

$$D = (m_{11}^2 - k^2 m_{22}^2) (\tan\beta - k). \quad (4)$$

where $k = \sqrt[4]{\lambda_1/\lambda_2}$. If $D < 0$ we live in a metastable state and our current (v_1, v_2) solution is the panic vacuum. We found panic points distributed all over the 2σ allowed region. We should note however that as shown in [20], the panic points are further away from the SM-like limit than the non-panic points.

In figure 3 we present similar plots to the ones shown in figure 1 the only difference being that all masses except for the lightest Higgs one are taken to be above 600 GeV. This plot is representative of the decoupling limit of the 2HDM - if all particles except h are too heavy to be detected at the LHC this is how the plot would look after the bounds on those masses are considered.

We finish this section with a comment on the values of M^2 and the values of the remaining masses that are still allowed by data. We had already noted that the points with $M^2 = 0$ are disallowed at 2σ in type I. We have checked that also $M^2 < 0$ is excluded at 2σ in type I. In type II all values of M^2 are allowed at 2σ . Regarding the remaining masses, our conclusion is that the data on the 125 GeV Higgs does not provide meaningful constraints on the masses of the remaining scalars.

A. Update after Moriond 2013

In this section we present updated plots after Moriond 2013. We use the latest updates from ATLAS [34] and from CMS [35] for the 7 and 8 TeV runs. Regarding the CMS results for $h \rightarrow \gamma\gamma$ we use the result from the Multivariate analysis.

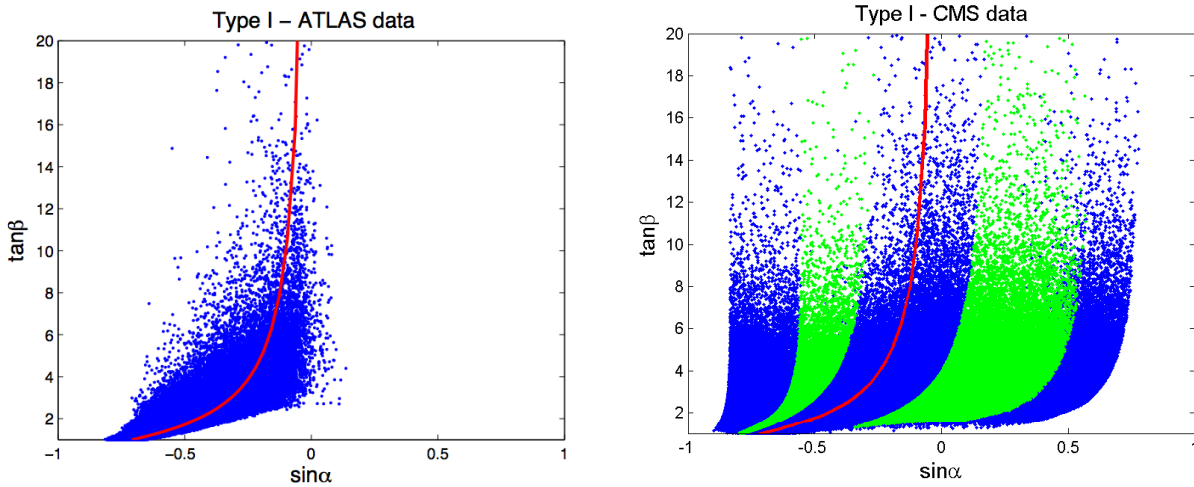


FIG. 4: Points in the $(\sin \alpha, \tan \beta)$ plane that passed all the constraints in type I using the ATLAS data (left) and using the CMS data (right) at 1σ in green (light grey) and 2σ in blue (dark grey). Also shown is the line for the SM-like limit, $\sin(\beta - \alpha) = 1$.

In figure 4 we present the results for the type I model in the $(\sin \alpha, \tan \beta)$ plane using the ATLAS data (left) and the CMS data (right). The differences between the two plots are easy to understand. The ATLAS data forces R_{ZZ} to be large but as we have previously shown (equation 2) R_{ZZ} can never be above one in type I. Consequently, no points survive at 1σ . With the CMS data plenty of 1σ points survive because all R_{VV} are below one. As expected, the 1σ region is slightly away from the SM-like limit because, on one hand, the central values of R_{VV} are below one, and, on the other hand, we already saw that R_{VV} are very sensitive quantities in type I.

In figure 5 we now show similar plots for the type II model. In type II R_{VV} is not a sensitive quantity. Therefore both the 1σ and the 2σ points are very close to the two limiting lines (in red). The difference between the two plots is that the points tend to concentrate below the limiting lines for ATLAS and above the same lines for CMS. This is of course a consequence of the central values of the ATLAS R_{VV} being above the SM while the CMS ones are below the SM expectation. Finally we present in figure 6 plots similar to the ones in figure 5 but now in the $(\cos(\beta - \alpha), \tan \beta)$ plane. Again we see the same trend with the allowed points on opposite sides of the limiting lines, $\cos(\beta - \alpha) = 0$ and $\cos(\beta + \alpha) = 0$.

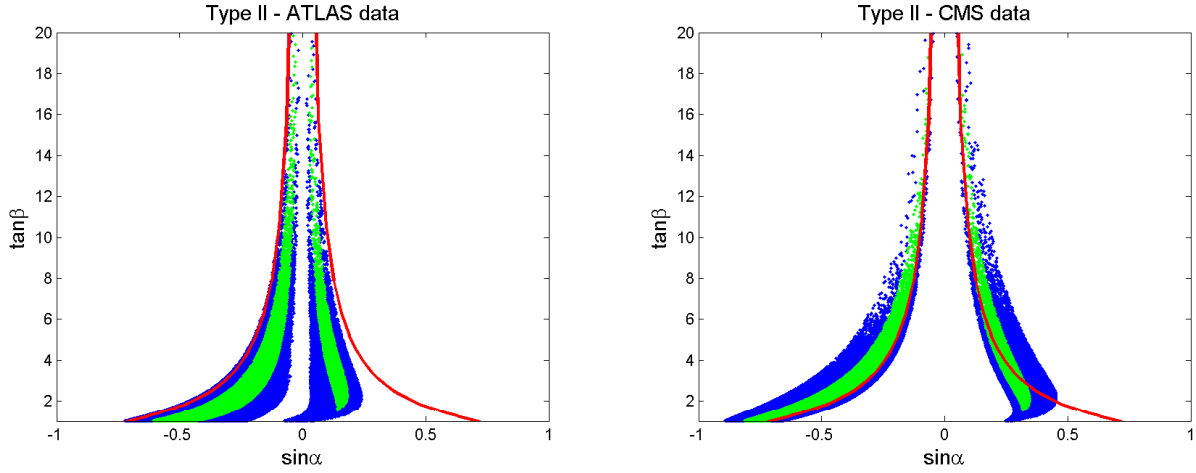


FIG. 5: Points in the $(\sin \alpha, \tan \beta)$ plane that passed all the constraints in type II using the ATLAS data (left) and using the CMS data (right) at 1σ in green (light grey) and 2σ in blue (dark grey). Also shown are the lines for the SM-like limit, that is $\sin(\beta - \alpha) = 1$ (negative $\sin \alpha$) and for the limit $\sin(\beta + \alpha) = 1$ (positive $\sin \alpha$).

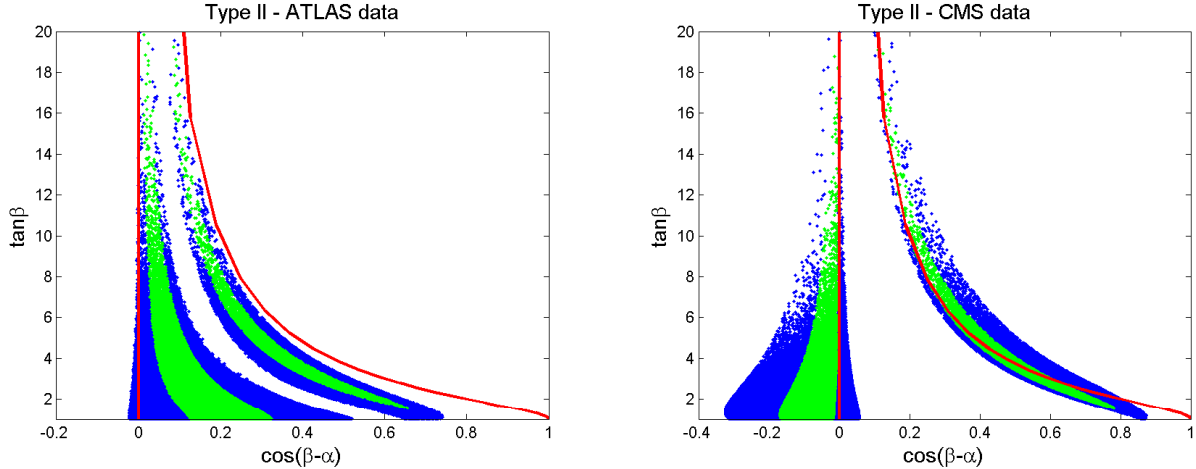


FIG. 6: Points in the $(\cos(\beta - \alpha), \tan \beta)$ plane that passed all the constraints in type II using the ATLAS data (left) and using the CMS data (right) at 1σ in green (light grey) and 2σ in blue (dark grey). Also shown are the lines for the SM-like limit, that is $\cos(\beta - \alpha) = 0$ and for the limit $\cos(\beta + \alpha) = 0$.

IV. CP-VIOLATING MODEL

In this section we discuss the CP-violating model 2HDM presented in section II. The lightest neutral particle of the model h_1 is considered to be the one discovered at the LHC. This particle can be seen as being composed by a CP-even and a CP-odd component. The amount of mixing is controlled by $s_2 = \sin \alpha_2$ (one of the three rotation angles in the neutral sector - see [6] for details). When $s_2 = 0$, h_1 is a pure CP-even state and when $s_2 = 1$, h_1 is a pure CP-odd state. Our goal is to constrain the amount of mixing using LHC data. In the left panel of figure 7 we show R_{ZZ} versus $R_{\gamma\gamma}$ for type I and for three regions of the parameter s_2 : $|s_2| < 0.1$ in green (light grey), $0.45 < |s_2| < 0.55$ in blue (black), and $|s_2| > 0.83$ in red (dark grey). In the right panel we present a similar plot for type II. We also show in both plots the combined ATLAS and CMS results at 1σ (yellow line) and at 2σ in blue. We conclude that the red points are excluded at 2σ when the combined results [32] from ATLAS and CMS are considered.

The results of the Moriond updates are shown as 2σ solid (CMS) and dashed (ATLAS) lines in figure 7. We see that $|s_2| > 0.83$ is still excluded at 2σ by the ATLAS data, but that it is allowed by the new CMS data.

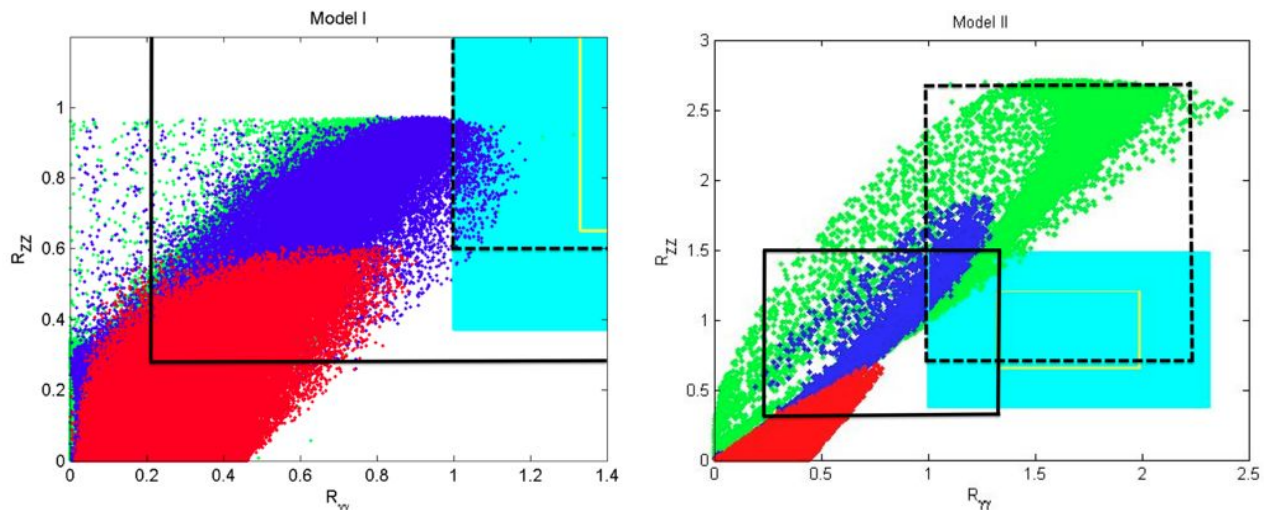


FIG. 7: In the left panel we show R_{ZZ} versus $R_{\gamma\gamma}$ for type I and for three regions of the parameter s_2 : $|s_2| < 0.1$ in green (light grey), $0.45 < |s_2| < 0.55$ in blue (black) and $|s_2| > 0.83$ in red (dark grey). In the right panel we present a similar plot for type II. We show in both plots the combined ATLAS and CMS results at 1σ (yellow line) and at 2σ in blue and the 2σ updated lines after Moriond 2013 (solid black - CMS and dashed black - ATLAS).

V. CONCLUSIONS

We have considered the most common CP-conserving 2HDMs and a CP-violating 2HDM in light of the recent data from the LHC. For the CP conserving case, there are 4 different models, corresponding to the transformation properties of the quarks, leptons and Higgs bosons under a Z_2 symmetry. We include constraints from vacuum stability, unitarity, precision electroweak constraints, LEP experimental bounds, bounds from b decays as well as LHC bounds on top decays. The full parameter space is scanned, subject to these constraints, and allowed points are plotted in the $(\sin\alpha, \tan\beta)$ plane and in the $(\sin\alpha, \cos(\beta - \alpha))$ plane. This talk was presented before the Moriond 2013 meeting, at which time the Standard Model branching ratios disagreed by more than one sigma with the combined data from ATLAS and CMS, and thus the plots show no points within one sigma of the Standard Model curves. However, we have updated the plots since Moriond, and find that in type I CMS data does allow points within one sigma of the Standard Model. In type II both ATLAS and CMS now allow points within one sigma of the SM. In the next run, these experimental bounds will tighten considerably, providing a strong test of the models.

In the CP violating case, the key parameter is s_2 , which controls the amount by which the observed 125 GeV state is CP-even vs. CP-odd. We have shown that some regions of relatively large s_2 can be excluded, but a wide range of values remains. Over the next few years, the rectangles shown in figure 7 will shrink considerably, providing a much stronger bound on the amount of the scalar's CP-odd component.

Acknowledgments

RS is grateful to the workshop organisation for financial support and for providing the opportunity for very stimulating discussions. The work of AB, PMF and RS is supported in part by the Portuguese *Fundação para a Ciência e a Tecnologia* (FCT) under contract PTDC/FIS/117951/2010, by FP7 Reintegration Grant, number PERG08-GA-2010-277025, and by PEst-OE/FIS/UI0618/2011. The work of JPS is funded by FCT through the projects CERN/FP/109305/2009 and U777-Plurianual, and by the EU RTN project Marie Curie: PITN-GA-2009-237920. The work of MS is supported by the NSF under Grant No. PHY-1068008.

-
- [1] G. Aad *et al.* [ATLAS Collaboration], Phys. Lett. B **716**, 1 (2012) [arXiv:1207.7214 [hep-ex]].
 [2] S. Chatrchyan *et al.* [CMS Collaboration], Phys. Lett. B **716**, 30 (2012) [arXiv:1207.7235 [hep-ex]].
 [3] P. M. Ferreira, R. Santos, M. Sher, J. P. Silva, Phys. Rev. D **85**, 077703 (2012) [arXiv:1112.3277 [hep-ph]].

- [4] P. M. Ferreira, R. Santos, M. Sher, J. P. Silva, Phys. Rev. D **85**, 035020 (2012) [arXiv:1201.0019 [hep-ph]].
- [5] G. Burdman, C. E. F. Haluch, R. D. Matheus, Phys. Rev. D **85**, 095016 (2012) [arXiv:1112.3961 [hep-ph]].
- [6] A. Barroso, P. M. Ferreira, R. Santos, J. P. Silva, Phys. Rev. D **86**, 015022 (2012) [arXiv:1205.4247 [hep-ph]].
- [7] V. D. Barger, J. L. Hewett and R. J. N. Phillips, Phys. Rev. D **41** (1990) 3421.
- [8] M. Aoki, S. Kanemura, K. Tsumura and K. Yagyu, Phys. Rev. D **80** (2009) 015017.
- [9] G. C. Branco, P. M. Ferreira, L. Lavoura, M. N. Rebelo, M. Sher and J. P. Silva, Phys. Rept. **516** (2012) 1 [arXiv:1106.0034 [hep-ph]].
- [10] P. M. Ferreira, R. Santos and A. Barroso, Phys. Lett. B **603** (2004) 219 [Erratum-ibid. B **629** (2005) 114]; A. Barroso, P. M. Ferreira, R. Santos, Phys. Lett. B **632**, 684 (2006) [hep-ph/0507224]; M. Maniatis, A. von Manteuffel, O. Nachtmann, F. Nagel, Eur. Phys. J. C **48**, 805 (2006) [hep-ph/0605184].
- [11] I. P. Ivanov, Phys. Rev. D **75**, 035001 (2007) [Erratum-ibid. D **76**, 039902 (2007)] [hep-ph/0609018]; I. P. Ivanov, Phys. Rev. D **77**, 015017 (2008) [arXiv:0710.3490 [hep-ph]].
- [12] I. F. Ginzburg, M. Krawczyk and P. Osland, hep-ph/0211371.
- [13] A. W. El Kaffas, W. Khater, O. M. Ogreid and P. Osland, Nucl. Phys. B **775** (2007) 45 [hep-ph/0605142].
- [14] A. Arhrib, E. Christova, H. Eberl and E. Ginina, JHEP **1104** (2011) 089.
- [15] N.G. Deshpande and E. Ma, Phys. Rev. D **18** (1978) 2574.
- [16] S. Kanemura, T. Kubota and E. Takasugi, Phys. Lett. B **313** (1993) 155; A.G. Akeroyd, A. Arhrib and E.M. Naimi, Phys. Lett. B **490** (2000) 119.
- [17] M.E. Peskin and T. Takeuchi, Phys. Rev. D **46**, 381 (1992).
- [18] H.E. Haber, “Introductory Low-Energy Supersymmetry,” in *Recent directions in particle theory: from superstrings and black holes to the standard model*, Proceedings of the Theoretical Advanced Study Institute (TASI 92), Boulder, CO, 1–26 June 1992, edited by J. Harvey and J. Polchinski (World Scientific Publishing, Singapore, 1993) pp. 589–688; C. D. Froggatt, R. G. Moorhouse and I. G. Knowles, Phys. Rev. D **45**, 2471 (1992); W. Grimus, L. Lavoura, O. M. Ogreid and P. Osland, Nucl. Phys. B **801**, 81 (2008) [arXiv:0802.4353 [hep-ph]]; H.E. Haber and D. O’Neil, Phys. Rev. D **83**, 055017 (2011) [arXiv:1011.6188 [hep-ph]].
- [19] I. P. Ivanov, Phys. Rev. E **79**, 021116 (2009).
- [20] A. Barroso, P. M. Ferreira, I. P. Ivanov, R. Santos, J. P. Silva, arXiv:1211.6119 [hep-ph]; A. Barroso, P. M. Ferreira, I. P. Ivanov, R. Santos, arXiv:1303.5098 [hep-ph].
- [21] G. Abbiendi *et al.* [ALEPH and DELPHI and L3 and OPAL and The LEP working group for Higgs boson searches Collaborations], [arXiv:1301.6065 [hep-ex]].
- [22] A. Denner, R.J. Guth, W. Hollik and J.H. Kuhn, Z. Phys. C **51**, 695 (1991). H.E. Haber and H.E. Logan, Phys. Rev. D **62**, 015011 (2000) [hep-ph/9909335]. The ALEPH, CDF, D0, DELPHI, L3, OPAL, SLD Collaborations, the LEP Electroweak Working Group, the Tevatron Electroweak Working Group, and the SLD electroweak and heavy flavour Groups, arXiv:1012.2367 [hep-ex]. F. Mahmoudi and O. Stal, Phys. Rev. D **81**, 035016 (2010) [arXiv:0907.1791 [hep-ph]]; M. Baak, M. Goebel, J. Haller, A. Hoecker, D. Ludwig, K. Moenig, M. Schott and J. Stelzer, Eur. Phys. J. C **72**, 2003 (2012) [arXiv:1107.0975 [hep-ph]]. M. Baak, M. Goebel, J. Haller, A. Hoecker, D. Kennedy, R. Kogler, K. Moenig, M. Schott and J. Stelzer, arXiv:1209.2716 [hep-ph]. A. Wahab El Kaffas, P. Osland, O. M. Ogreid, Phys. Rev. D **76**, 095001 (2007) [arXiv:0706.2997 [hep-ph]]; L. Basso, A. Lipniacka, F. Mahmoudi, S. Moretti, P. Osland, G. M. Pruna, M. Purmohammadi, JHEP **1211**, 011 (2012) [arXiv:1205.6569 [hep-ph]].
- [23] D. Asner *et al.* [Heavy Flavor Averaging Group Collaboration], arXiv:1010.1589 [hep-ex]. T. Hermann, M. Misiak and M. Steinhauser, JHEP **1211** (2012) 036. See also, F. Mahmoudi, talk given at Prospects For Charged Higgs Discovery At Colliders (CHARGED 2012), 8-11 October, Uppsala, Sweden.
- [24] G. Aad *et al.* [ATLAS Collaboration], JHEP **1206** (2012) 039 [arXiv:1204.2760 [hep-ex]].
- [25] S. Chatrchyan *et al.* [CMS Collaboration], JHEP **1207** (2012) 143 [arXiv:1205.5736 [hep-ex]].
- [26] S. Schael *et al.* [ALEPH and DELPHI and L3 and OPAL and LEP Working Group for Higgs Boson Searches Collaborations], Eur. Phys. J. C **47**, 547 (2006) [hep-ex/0602042].
- [27] J.P. Lees *et al.* [BaBar Collaboration], Phys. Rev. Lett. **109**, 101802 (2012) [arXiv:1205.5442 [hep-ex]].
- [28] M. Spira, arXiv:hep-ph/9510347.
- [29] https://twiki.cern.ch/twiki/bin/view/LHCPhysics/CrossSectionsFigures#Higgs_production_cross_sections
- [30] R.V. Harlander and W.B. Kilgore, Phys. Rev. D **68**, 013001 (2003) [hep-ph/0304035].
- [31] C. -W. Chiang and K. Yagyu, arXiv:1303.0168 [hep-ph].
- [32] A. Arbey, M. Battaglia, A. Djouadi, F. Mahmoudi, Phys. Lett. B **720**, 153 (2013) [arXiv:1211.4004 [hep-ph]].
- [33] B. Gorcezyca, M. Krawczyk and , arXiv:1112.5086 [hep-ph].
- [34] The ATLAS collaboration, ATLAS-CONF-2013-012, ATLAS-CONF-2013-013, ATLAS-CONF-2013-030, ATLAS-CONF-2013-034.
- [35] The CMS collaboration, CMS notes CMS-PAS-HIG-13-001, CMS-PAS-HIG-13-002, CMS-PAS-HIG-13-003 and CMS-PAS-HIG-13-003.